Impact assessment of cadmium chloride on human cell lines and yeast knockout strains

Shimaa A.A. Mousa[a], Abd El-Hamid A. Haggran[a], Tahany M.A. El-Kawokgy[a], Zakia A. Abo El-Kheir[b], Shadia M.H. Sabry[b], Shimaa E. Rashad[a]

[a]Department of Microbial Genetics, Biotechnology Research Institute, National Research Center, Giza, [b]Department of Botany and Microbiology, Faculty of Science, Al-Azhar University (Girls Branch), Cairo, Egypt

Correspondence to Shimaa A.A. Mousa, M.Sc. Sci. Microbial Genetics, National Research Center, 33 El-bohoth st., Giza, Egypt.
E-mail: Sa.Mousa@nrc.sci.eg, shimaa_abdellatif@yahoo.com

Received: 22 June 2022
Revised: 29 July 2022
Accepted: 29 July 2022
Published: xx Month 2022

Egyptian Pharmaceutical Journal 2022, 21:447–455

Background
Cadmium (Cd) is a heavy metal that contributes to pollution in the environment. Cd intoxication can lead to diseases in the liver, kidneys, and lungs, among other organs. The liver is the primary organ affected by Cd overdose.
Objective
To evaluate the cytotoxic and genotoxic responses of cadmium chloride ($CdCl_2$) on three different human cell lines and four different genotypes of yeast knockout strains.
Materials and methods
The effects of different concentrations of $CdCl_2$ on cell viability in hepatocellular carcinoma (HepG2), lung cancer (A549), and normal lung cell carcinoma (Wi38) were investigated systematically using the MTT method. Moreover, flow cytometry was used to assess cell cycle arrest using propidium iodide (PI) staining and to quantify apoptotic cell death using PI staining and Annexin V/PI staining, respectively. The gene expression of p53, casp3, and Bcl-2 was measured using qRT-PCR. The Comet methodology was used to indicate DNA damage of yeast knockout strains.
Results and conclusion
The MTT assay revealed that $CdCl_2$ was highly potent against hepatocellular carcinoma (HepG2), lung cancer (A549), and normal lung cell lines (Wi38) (IC50=3.12, 28.81, 191.14 μg/ml). These findings showed that $CdCl_2$ reduced therapeutic efficacy in malignant cells at relatively low concentrations compared with nonmalignant cells, as well as confirmed the antitumor effect of the metal. $CdCl_2$-damaged A549 cells revealed a significant increase in arrest of cell cycle in 'S' phases, and then apoptosis increased. Subsequently, when A549 cells were treated with a higher dosage of $CdCl_2$, the gene expression of p^{53} and casp3 genes was upregulated, whereas Bcl-2 was downregulated. $CdCl_2$ revealed its genotoxic activity at different concentrations of 10, 25, 50 μg/ml. *MRE11*, *CLN1* and *ZRC1* genes exhibited marked genotoxic effects, while *MMT1* gene generated modret genotoxicity of yeast knockout strains. The Comet assay revealed that yeast cells were more responsive, which was indisputably demonstrated.

Keywords:
apoptosis, cadmium chloride, comet assay, hepatocellular carcinoma (HepG2), lung cancer (A549), MTT assay, normal lung cell carcinoma (Wi38)

Egypt Pharmaceut J 21:447–455

1687-4315

Introduction

Cadmium (Cd) is a metallic element that has no biological functions and is frequently regarded as a toxin [1,2]. The use of Cd as a corrosive chemical in industry, nickel–Cd rechargeable battery, a stabilizer in polyvinyl chloride, polyvinyl chloride materials, and color compounds, are all constant sources of Cd pollution [3]. House dust is a potential pathway for carcinogens in locations with polluted soils [4]. Nickel and copper refining and smelting, burning of fossil fuel, and the phosphate fertilizers are all anthropogenic sources of Cd in the environment. Cd is however found as a contaminant in nonferrous metal heavy industries and technological recycling and reuse. Increases in Cd concentration range in the living situation (atmosphere, soil, and water) are caused by volcanic activity, the diminishment and irritation of rocks and soil, and forest fires; even mines lead, zinc, and copper make a contribution to the discharge of this compound to atmosphere, and contaminated soil as resulted [5]. Cd is absorbed mostly via the respiratory tract and to a lesser degree through the gastrointestinal tract, with absorption of skin being uncommon. Slow

Cd excretion from the body is via the saliva, urine, and milk lactation. In human, Cd exposure leads to unfavorable effects, such as hepatic and renal damages, testicular damage, and aspiratory edema [6]. Cd carcinogenic elements are induced mostly through the oxidative stress, decreased apoptosis, DNA damage, and diminished DNA repair capacity [7–9].

Chronic heavy metal consumption, in particular, triggers an adaptation mechanism to excessive pressure, but acute heavy metal inebriation has the opposite effect. In fact, if cells subjected to elevated Cd doses for a short time (acute exposure), they may go into the apoptotic process and have a lower metastatic capacity, whereas chronic pattern causes transformation of normal epithelial cells to malignant as a result of an adjustment process characterized by resistance to apoptosis, increased invasion capacity, and dedifferentiation characteristics [10]. In 2020, lung cancer was the most common second diagnosed cancer and considered a major cause of death. Moreover, liver cancer is the sixth most common diagnosed cancer and the third leading cause of death worldwide [11].

Rashad [12] discovered that some compounds that entered in foods reduced cell proliferation in both malignant and nonmalignant cells, confirming the cytotoxic activity, and they have been shown to be more responsive in *Saccharomyces cerevisiae* cells. The Comet assay was used to investigate the consequences of chemicals on multiple yeast haploid knockout strains to determine the optimum quantities at which this combination of dietary chemicals could cause DNA damage [13]. Cd causes renal cancer and is known to inactivate p53. G2/M arrest contributes to stabilization of p53-deficient mutated cells. Moreover, the comet assay experiments showed that Cd (50–100 μM) induced DNA damage within 1–6 h [14].

Materials and methods

Cell lines

Mammalian cell lines

The American Type Culture Collection provided A549 cells (human lung carcinoma), HepG2 cells (human hepatocellular carcinoma), and Wi38 cells (human lung fibroblast normal cells) (ATCC, Rockville, Madison, USA).

Chemicals used

Sigma provided the dimethyl sulfoxide (DMSO), MTT, and trypan blue dye used in this study (St Louis, Missouri, USA).

Lonza provided fetal cattle serum, 1640-RPMI, L-glutamine, gentamycin, HEPES solution buffer, and 0.25% EDTA-Trypsin (Belgium).

Cell line proliferation

The cells were cultivated on RPMI-1640 media supplemented with 10% inactivated fetal cattle serum plus 50 μg/ml gentamycin. The cells were subcultured two to three times a week and kept at 37°C of 5% CO_2.

Evaluation of cytotoxicity using MTT assay

Antimutagenic assay: the malignant cell lines were interrupted in the medium concentrations of 5×10^4 cells/well of Corning 96-well culture cell plates, followed by incubation for 1 day. After that, different Cd concentrations were applied to 96-well plates (three replicates). As a control, each 96-well plate was run with 0.5% DMSO. The MTT test was used to assess the amount of viable cells after a 24-h incubation period. In brief, the medium was replaced from the 96-well plates with 100 μl of pure culture RPMI-1640 medium without phenol red and 10 μl of 12 mM MTT stock solution [5 mg of MTT in 1 ml phosphate buffered saline (PBS)] to each well, including control. The 96-well cultures were maintained for 4 h at 37°C with 5% CO_2. An 85 μl of the media was removed from the wells, and 50 μl of DMSO was added to each well. All wells were properly mixed by a pipette before incubation of 37°C for 10 min. The optical density was measured at 590 nm with the microplate reader (Sunrise, Morrisville, North Carolina, USA, TECAN, lnc. Company) to determine the number of viable cells, and the significant proportion of viability was calculating by [(ODt/ODc)]×100%, where ODt means optical density of the tested sample, and ODc means optical density of the untreated cells. The survival curve of all cell lines following treatment of the prescribed tested compounds was displayed using the relationship between surviving cells and Cd concentrations. The 50% of inhibited concentration (IC50), defined as the concentration to elicit harmful effects at 50% of intact cells, was calculated using plots graphic of dose–response curve for each concentration (San Diego, California, USA) [15].

Flow cytometry

Cell cycle analysis by propidium iodide assay using flow cytometry

Trypsin–EDTA (warm) and PBS–EDTA (warm) (500 μl+500 μl) were used to digest the cells, which were incubated at 37°C for 10 min. After centrifuging the mixture for 5 min at 400 rpm, the supernatant was

removed carefully. The cell pellet was resuspended in 500 µl PBS (warm) and centrifuged, and the supernatant was removed after the mixture was washed twice in warm PBS. To fix the cells, a volume of 150 µl PBS and 350 µl ice cold 70% ethanol was added and incubated for 1 h at 4°C. The mixture was centrifuged for 10 min at 350 rpm to remove the ethanol, and then the supernatant was removed carefully. The cells were resuspended in 500 µl of warm PBS after being washed twice in PBS and centrifuged, and the precipitate was extracted. The cells were resuspended in 100 µl of PBS and at 4°C kept in the dark for up to 4 days. The cells were stained with 100 µl of propidium iodide (PI) solution, and then 50 µl of RNase A solution (100 µg/ml) was added and incubated for 30–60 min in dark [15]. The labelled samples were characterized in cast spell flow cytometry (Applied Bio-system, USA).

Apoptosis analysis by Annexin V-FITC Assay using flow cytometry

Overall, $1–5\times10^5$ cells were collected, and the supernatant was discarded. After that, the cells were harvested, washed repeatedly in PBS warm buffer, and reconstituted in 500 µl of 1× binding buffer. Then, they were incubate for 5 min at room temperature in dark with 5 µl of Annexin V-FITC plus 5 µl of PI 50 mg/ml [16]. Flow cytometry was used to examine Annexin V-FITC interaction (Applied Bio-system).

Quantitative real time PCR analysis

The Gene JET RNA Purification Kit (# K0731; Thermo Scientific, USA) was used to extract total RNA from A549 cells according to manufacturer's instructions. Revert Aid H Minus Reverse Transcriptase (#EP0451; Thermo Scientific) was used to reverse transcribe total RNA (5 µg) to cDNA, as previously described [16]. As a template, the cDNA was employed to assess the relative expression of genes related to apoptosis (Applied Bio-system). Primer 5.0 software was used to design the primers. Casp3, Bcl-2, p^{53}, and GAPDH reverse and forward primer sequences are shown in Table 1.

To determine the fold change in gene expression of the target genes, the housekeeping GAPDH gene was used as a reference. Overall, 12.5 µl of 2× Maxima SYBR Green/ROX qPCR MM (# K0221; Thermo Scientific), 2 µl of cDNA template, 1 µl reverse primer, 1 µl forward primer, and 8.5 µl of nuclease-free water were combined to make a 25 µl PCR mix. The cycling program started with denaturation at 95°C for 10 min, then 40–45 cycles of DNA amplification at 95°C for 15 s, followed by annealing at 60°C for 30 s, and extension at 72°C for 30 s. For melting curve analysis, the temperature was increased from 63 to 95°C at the end of the previous cycle. The cycling threshold (Ct) levels for target genes and the housekeeping gene were obtained, and differential expression has been measured using the $2^{-\Delta\Delta Ct}$ technique [17].

Yeast comet assay

The initial approach published was used to accomplish the *in vitro* Comet assay [13]. We employed Cd doses of 10, 25, and 50 µg/ml in yeast culture media. As an untreated control, a medium devoid of chemical components was used. About 1 g of cell pellets was mixed with cold PBS in a 1 cm^3 container. The suspension was filtered after stirring for 5 min. A total of 100 µl of cell solution and 600 µl of low melting agarose were mixed. Overall, 100% of this combination was spread out on precoated slides. The coated slides were submerged in lyses buffer for 15 min (0.045 M TBE, pH 8.4, containing a pair of 0.5% SDS). Coated slides were placed in the electrophoresis tank filled with electrophoresis buffer at 4°C and an electric field of 2 V/cm for 15 min neutralization buffer was used to neutralize the microgels at room temperature for 10 min, and then excess of neutralization buffer was drained from the samples by 76 and 96% ethanol, respectively, for 10 min at room temperature. Each slide was stained by 50 µl of ethidium bromide (20 mg/m1) staining. While the samples still moist, the polymeric fragment migration pathways of 100 cells for each levels of exposure were evaluated with a visible radiation magnifier [with stimulation filter 420–490 nm (issue 510 nm)]. Extraterrestrial object tail lengths were measured from nucleus to top of the tail. To visualize polymer damage, a 40× objective on a fluorescence magnifier was used to observe Gel Red-

Table 1 The casp3, bcl-2, p^{53}, and GAPDH genes' reverse and forward primer sequences

Genes	Forward primer (5' - 3')	Reverse primer (5' - 3')
Casp3	TTCATTATTCAGGCCTGCCGA	TTCTGACAGGCCATGTCATC
Bcl-2	CATGCAAGAGGGAAACACCA	GTGCTTTGCATTCTTGATGA
p^{53}	AGAGTCTATAGG CCACCCC	GCTCGACGCTAGGATCTGAC
GAPDH	TGCACCACCAACTGCTTAGC	GGCATGGACTGTGGTCATGA

stained polymers. An interplanetary object five image processing code established by Kinetic Image Processing Ltd (Liverpoo1, UK) connected to CCD camera was used to evaluate the quantitative and subjective extent of polymer injury within the cells by measuring the polymer migration length and the percentage of transitioned polymer. The tail moment was then calculated by the software. In most cases, 50–100 randomly selected cells per sample were analyzed [13].

Knockout yeast strains of choice

In this study, haploid deletion strains with fully different genotypes have been employed, and the sequence within each strain were selected and aligned with human sequence data in The National Center for Biotechnology Information. According to the findings, four genes linked with cancer-related human genes were chosen to match with the yeast genes employed in this study [18] (Table 2).

Selection of yeast haploid strains deficient in genes similar to human cancer genes

The genotyping of saccharomyces haploid (gene deletion) strain was determined based on similarity between human and yeast genes (Clustal Omega Multidisciplinary Homology Modeling EMBL-EBI), according to Mousa *et al.* [18].

Statistical analysis

The data were all reported as means with SD. One-way analysis of variance was used to determine statistical significance, and Duncan's multiple range test was used to determine individual comparisons (DMRT). When P value of 0.05, results were considered to be significant.

Results and discussions

Cytotoxic effect using MTT assay

The MTT cytotoxic test was used to assess the cytotoxic effects of cadmium chloride ($CdCl_2$) at various doses on the development of HepG2, A549, and Wi38 cells in contrast to a positive reference. As the quantities of $CdCl_2$ increased, cell viability decreased steadily, as seen in Table 3. Regarding cell survival and cytotoxicity as the tested $CdCl_2$ concentration grew, the viability of the positive control decreased. Table 3 lists the doses that cause 50% of cell growth inhibition (IC50) in hepatoma cell lines (HepG2), as well as $CdCl_2$ concentration curve for viable cells (Fig. 1).

As the quantities of $CdCl_2$ increased, cell viability decreased steadily, as seen in Table 4. Regarding $CdCl_2$ cytotoxicity and cell survival, as the concentration of tested $CdCl_2$ increased, the viability of the positive control decreased. Table 4 shows the dose that causes 50% of cell inhibitory activity (IC50) in lung cell lines (A549), as well as dosage curves for treated cells in Fig. 2.

As the quantities of $CdCl_2$ increased, cell viability decreased steadily, as seen in Table 5. Cd's cytotoxicity increased and cell survival decreased as the concentration of $CdCl_2$ increased. Table 5 shows the dose that causes 50% of cell inhibitory activity (IC50) in normal lung cell lines (Wi38), as well as

Table 2 Yeast genes that resembled cancer-related human genes were chosen

Selected strains	Selected genes of yeast strains (genotypes)	Homologous genes in human
YMR177W	MMT1	SLC30A9
YMR199W	CLN1	CCNA1
YMR224C	MRE11	MRE11
YMR243C	ZRC1	SLC30A10

Table 3 Varied cadmium chloride concentrations have different effects on hepatocellular carcinoma cells (HepG2)

$CdCl_2$ concentration (μg/ml)	%Viability	%Inhibitory	SD (±)
500	1.35	98.65	0.17
250	4.68	95.32	0.42
125	9.73	90.27	0.69
62.5	14.08	85.92	0.74
31.25	18.29	81.71	0.87
15.6	26.74	73.26	1.42
7.8	34.59	65.41	2.35
3.9	42.78	57.22	1.94
2	59.13	40.87	2.31
1	70.46	29.54	1.82
0	100	0	0

$CdCl_2$, cadmium chloride.

Figure 1

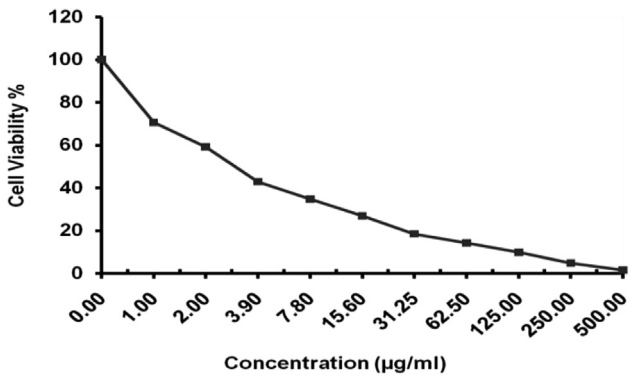

$CdCl_2$ concentrations have inhibitory action against hepatocellular cancer cells (HepG2). $CdCl_2$, cadmium chloride.

Table 4 Varied cadmium chloride concentrations have different effects on lung cancer cells (A549)

$CdCl_2$ concentration (μg/ml)	Viability %	Inhibitory %	SD (±)
500	3.83	96.17	0.21
250	8.72	91.28	0.48
125	16.54	83.46	0.62
62.5	31.27	68.73	1.45
31.25	46.59	53.41	2.37
15.6	68.46	31.54	2.82
7.8	86.29	13.71	1.43
3.9	97.46	2.54	0.28
2	100	0	
1	100	0	
0	100	0	

$CdCl_2$, cadmium chloride.

Figure 2

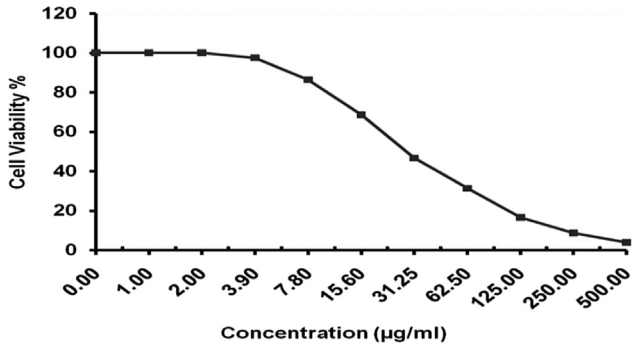

$CdCl_2$ concentrations have an inhibitory effect on lung cancer cells (A549). $CdCl_2$, cadmium chloride.

Table 5 Effects of the various cadmium chloride concentrations on normal human lung fibroblast cells (Wi38)

$CdCl_2$ concentration (μg/ml)	Viability %	Inhibitory %	SD (±)
500	14.69	85.31	1.47
250	36.23	63.77	2.81
125	65.29	34.71	3.17
62.5	86.41	13.59	1.73
31.25	98.62	1.38	0.84
15.6	100	0	
7.8	100	0	
3.9	100	0	
2	100	0	
1	100	0	
0	100	0	

$CdCl_2$, cadmium chloride.

$CdCl_2$ curve for cells treated in Fig. 3. It was discovered that A549 lung cancer cells were more susceptible to $CdCl_2$ than MRC-9 normal lung cells. Their LD50 levels mirrored the differences in their sensitivities. The IC50 of $CdCl_2$ for lung cancer cells was 87.5 μM, whereas the normal MRC-9 lung cells had IC50 of 112.5 μM. $CdCl_2$ concentration-dependent cell survivals were also found [19]. Moreover, EC50 value of 68.6 μM was determined, and the lowest

Figure 3

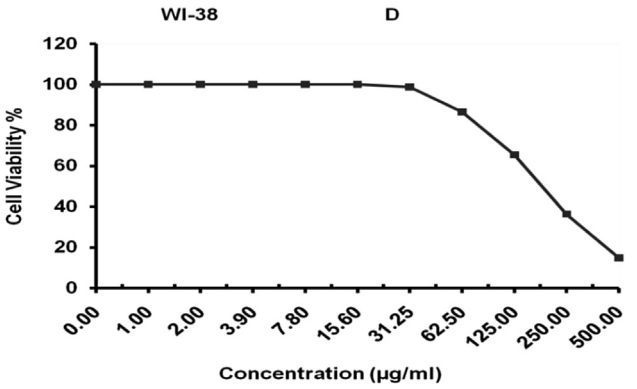

$CdCl_2$ concentrations have an inhibitory effect on human lung fibroblast normal cells (WI38). $CdCl_2$, cadmium chloride.

Table 6 Using A549 cells, the average percent of DNA content in each cell cycle phase was calculated

	Percentages of DNA content each in cell cycle phase			
Groups	G0/G1 phase	S phase	G2/M phase	Pre-G1
Cont.	49.91	44.16	5.93	1.19
$CdCl_2$	47.59	48.39	4.02	13.03

$CdCl_2$, cadmium chloride.

concentration of $CdCl_2$ that had a cytotoxic activity was 30 μM [20]. Following a 24-h dosing interval to 5, 10, 20, 40, 60, and 80 μM $CdCl_2$, a dosages curve of $CdCl_2$-induced cell death in BJAB cells for the 24-h exposure, the mean lethal concentration (LC50) was 40 μM [21].

Analysis of cell cycle by propidium iodide assay using flow cytometry

The DNA content of A549 cells was altered by 30 μg/ml $CdCl_2$. Control exhibited a reduction from 49.91 to 47.59% in the G0/G1 phase. Table 6 shows that when A549 cells were treated with $CdCl_2$, their DNA content increased by 48.39% compared with the control (44.16%) in the S phase. The cell cycle distribution of A549 cells was also influenced by $CdCl_2$ at 30 μg/ml. These findings revealed a high accumulation of induced apoptosis in the S phase, confirming that $CdCl_2$ has a strong lethal effect by inducing cell differentiation cycle arrest, as shown in Fig. 4. The observed increase in the G0/G1 phase of Cd-exposed cells could be explained by the mutagenic effect of Cd [7]. Moreover, Forti *et al.* [20] indicated that Cd induced G2 arrest and increased apoptosis.

Apoptosis analysis by Annexin V-FITC assay using flow cytometry

Apoptosis is a finely controlled process that is influenced by a number of signaling channels,

Figure 4

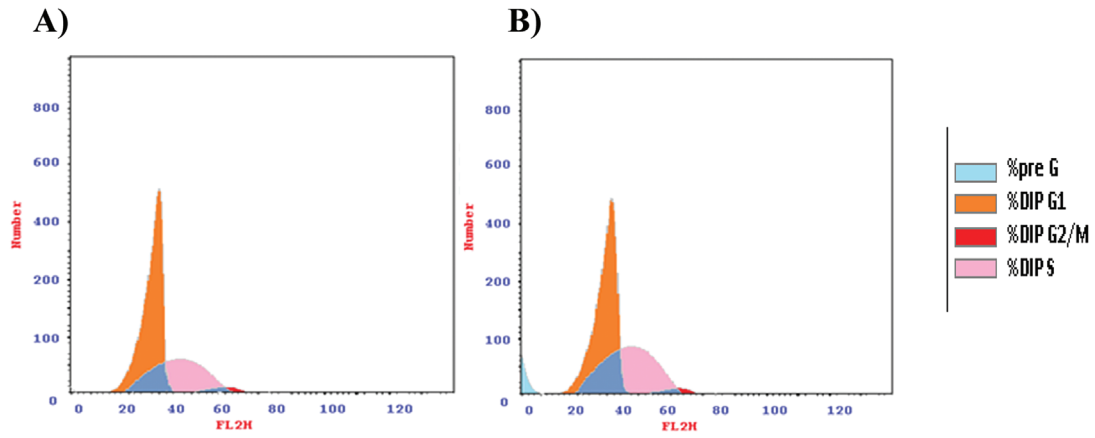

(a) Untreated lung cancer cell line (A549). (b) Treatment of lung cancer cell line (A549) with $CdCl_2$ (30 μg/ml) and effect on S cell cycle arrest. $CdCl_2$, cadmium chloride.

Figure 5

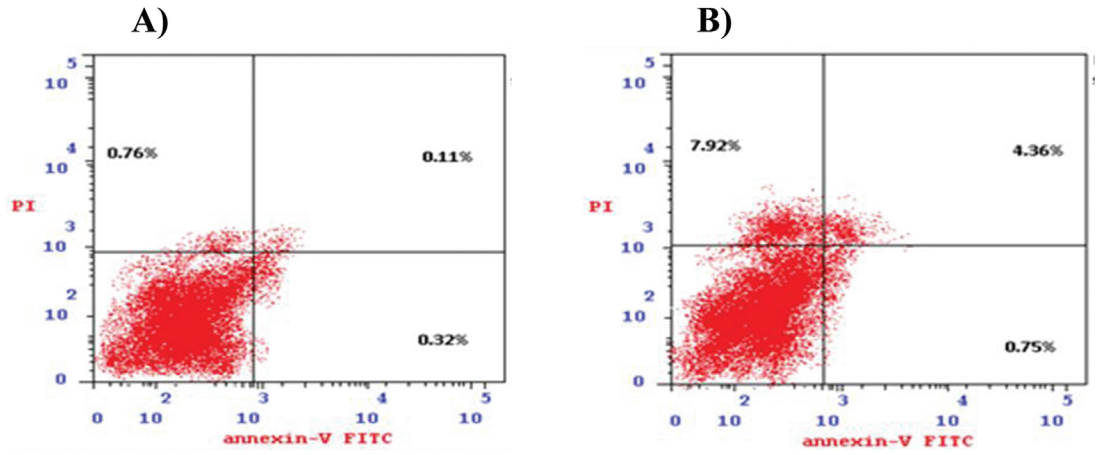

(a) Untreated cancerous cell line (A549). (b) Cancerous cell line (A549) treatment with $CdCl_2$ at a concentration of 30 μg/ml. Lower left (living cells)–lower right (early apoptosis)–upper right (late apoptosis)–upper left (necrotic cells). $CdCl_2$, cadmium chloride.

including the mitochondrial pathway and the caspase cascade. The effects of $CdCl_2$ at a concentration of 30 μg/ml on A549 cells were studied to assess cell necrosis and apoptosis. Flow cytometry with Annexin V-FITC/PI quintuple flow cytometry was used to detect apoptosis and necrosis (Fig. 5). The percentage of early and late apoptotic cells was used to compute the apoptotic rate. The apoptosis rate in $CdCl_2$-treated A549 cells was 0.75% for early apoptotic cells and 4.36% for late apoptotic cells, as shown in Table 7. For early and late apoptotic cells, the control was 0.32 and 0.11%, respectively. $CdCl_2$-treated A549 cells had a necrotic effect of 7.92%, whereas control cells had a necrotic effect of 0.76%. These findings revealed that $CdCl_2$ had substantial apoptotic cell influence on A549 cells. $CdCl_2$ induces apoptosis of HepG2 cells, compared with the control.

Table 7 Cadmium chloride treatment causes apoptosis and necrosis in A549 cells

	Percentage of apoptosis		
Group	Early	Late	Percentage of necrosis
A549-control	0.32	0.11	0.76
A549-tretedwith $CdCl_2$	0.75	4.36	7.92

$CdCl_2$, cadmium chloride.

There was a gradual increase of Annexin-positive cells in $CdCl_2$-treated cells [22].

Quantitative real-time PCR analysis genotoxicity induced by cadmium chloride for some related genes, casp3, Bcl-2, and p^{53}in A5493 cells

On lung cancer cell lines (A549), the function of apoptosis in $CdCl_2$-induced cytotoxicity was

Figure 6

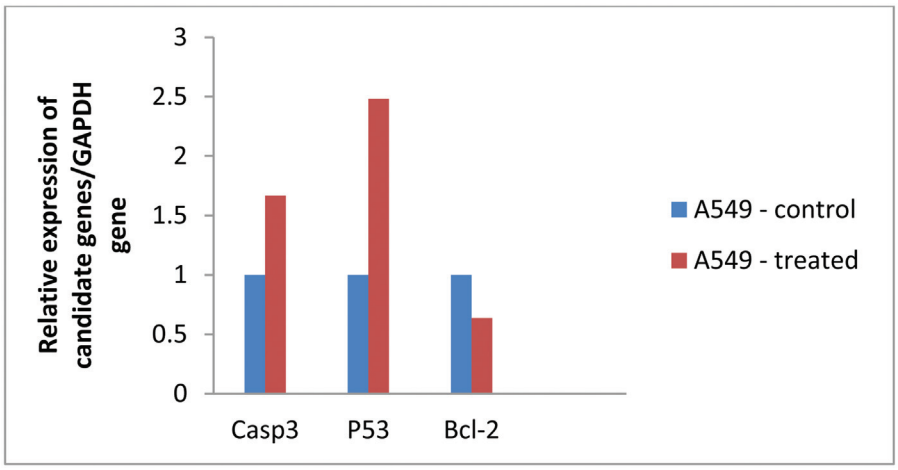

$CdCl_2$ effects on apoptosis-related genes after 30 μg/ml treatment, mRNA expression of casp3, p^{53}, and Bcl-2 was measured by conventional RT-PCR. *P value of 0.05, when compared with the control group. $CdCl_2$, cadmium chloride.

Table 8 The effect of the cadmium chloride compound on the relative expression of the casp3 gene in A549

Groups	Casp3 Ct values	ΔCt	ΔΔCt	Relative quantification
A549–control	33.26	9.74	0.00	1.00
A549 – treated	31.32	8.94	-0.8	1.66828662

Table 9 The influence of the cadmium chloride compound on the relative expression of the p53 gene in A549 cells

Groups	P53 Ct values	ΔCt	ΔΔCt	Relative quantification
A549–control	32.91	9.39	0.00	1.00
A549 – treated	31.14	7.97	-1.42	2.48044975

investigated. Real-time PCR was used to determine the expression levels of apoptotic related genes such casp3, p^{53}, and Bcl-2 in A549 cells. Figure 6 shows that Casp3 was upregulated by 1.66828662 fold change over control (Table 8), p^{53} was upregulated by 2.48044975 fold change over normal (Table 9), and Bcl-2 was down-regulated by 0.63494306 in the experimental group than in the control group (Table 10). These findings showed that $CdCl_2$ destroyed A549 cells by inducing apoptosis mostly through casp3 and p^{53} gene upregulation, with Bcl-2 being downregulated. This is similar to Ravindran *et al.* [23], who found that activation of p^{53} is essential for Cd-induced apoptosis and that inhibiting p^{53} activity reduced apoptosis in Cd-exposed cells. As a result, a cell without a functioning p^{53} gene is likely to be resistant to Cd-induced cell death. The antiapoptotic gene Bcl-2 was downregulated in HEK293 cells, whereas the pro-apoptotic gene Bax was upregulated, which is consistent of a cell undergoing programmed cell death. Cd inhibits p^{53} activity by decreasing its DNA adsorption affinity, resulting in defective DNA replication and Cd-induced carcinogenesis, according to Luevano and Damodaran [24].

Toxicity to yeast knockout strains tested with cadmium chloride by Comet assay

$CdCl_2$ was found to have genotoxic action at concentrations of 10, 25, and 50 μg/ml. The CLN1, MRE11, and ZRC1 genes were all shown to be genotoxic, although the genotoxicity of the MMT1 sequence was lower than that of the other genes. The pattern of percentages of observed comets for $CdCl_2$ is shown in Table 11. For each of the four examined genes, the yeast visualized considerably more comets than the respective control (Fig. 7), indicating that the tested chemical caused greater DNA damage. It was clear that $CdCl_2$ caused significant damage to all four genes evaluated. The comet assay revealed that all three concentrations had varying degrees of substantial genotoxic activity on yeast. Belliardo *et al.* [25] observed a significant difference in DNA strand breakage in normal epidermal cells starting at 100 μM $CdCl_2$. In the negative control cells that were not exposed to metals or chemicals, the average

Table 10 The effect of administering the cadmium chloride compound just on relative expression of the Bcl-2 genes in A549 cells

Groups	Bcl-2 Ct values	ΔCt	ΔΔCt	Relative quantification
A549–control	29.18	5.66	0.00	1.00
A549 – treated	29.54	6.37	0.71	0.63494306

Table 11 Imaging analysis was used to determine comet assay parameters in cells from all groups following cadmium chloride treatment

Concentrations	Tail length (px)	Tail DNA (%)	Tail moment	Tail olive moment
Control MMT1 (A)	3.2	16.42885	0.856675	1.331495
10 μg/m l (A1)	4.94	17.159516	1.5817580	2.04541
25 μg/ml (A2)	7.4	17.91486	2.422458	2.792965
50 μg/ml (A3)	8.68	24.05293	4.474314	4.154219
Control CLN1 (B)	4.14	17.84848	1.408786	2.093441
10 μg/m l (B1)	6.72	21.98804	2.292362	2.683942
25 μg/ml (B2)	11.08	24.37346	6.854292	5.379563
50 μg/ml (B3)	15.42	25.26561	8.687371	6.358607
Control MRE11 (C)	3.7	11.32471	0.644259	1.424435
10 μg/ml (C1)	6.77	24.24129	2.715358	3.169739
25 μg/ml (C2)	10.9	25.87569	5.691588	4.995281
50 μg/ml (C3)	14.5	34.86392	9.671687	7.376478
Control ZRC1 (D)	4.510204	15.1704	0.988069	1.662803
10 μg/ml (D1)	7.98	18.86137	3.144756	3.27737
25 μg/ml (D2)	13.14	29.64827	7.224068	6.019748
50 μg/ml (D3)	14.46	31.37756	7.687948	6.549478

Figure 7

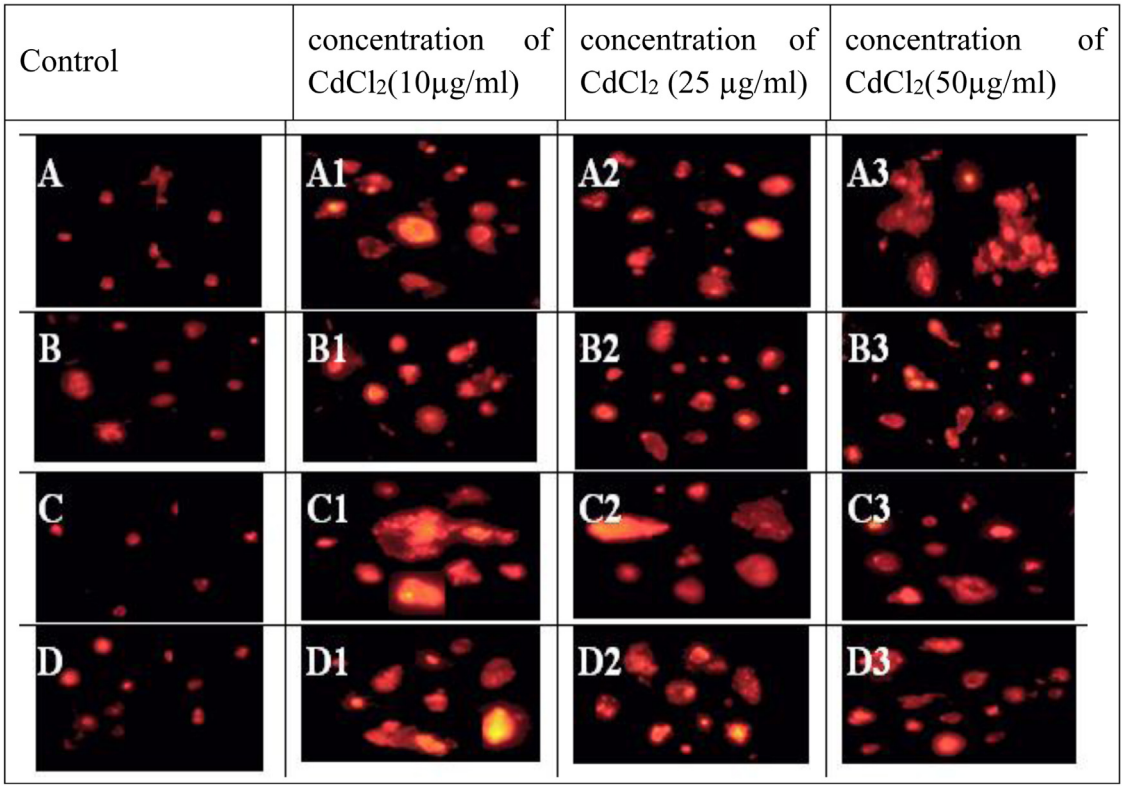

Using the Comet assay and $CdCl_2$ at a dosage of (10, 25, 50 μl/ml), photomicrographs of DNA damage in yeast strains were taken. Cells that act as a check A represents the control MMT1 gene; A1, A2, A3 represent the treated MMT1 gene; B represents the control CLN1 gene; B1, B2, B3 represent the treated CLN1 gene; C represents the control MRE11 gene; C1, C2, C3 represent the treated MRE11 gene; D represents the control ZRC1 gene; D1, D2, D3 represent the treated ZRC1 gene.

percentage of DNA damage was 0.58 [26]. The percentage of DNA damage caused by Cd was 6.24% at IC25 and 12.80% at IC30. The fact that the tail lengths of DNA comets were always longer in $CdCl_2$-treated cells than in control cells suggested that oxidative stress may play a role in $CdCl_2$-induced cyto/genotoxicity and death of HepG2 cells, particularly at higher levels of exposure [22].

Conclusion

$CdCl_2$ has been shown to successfully cause apoptosis in HepG2 cells. The activation of a mitochondria-mediated caspase cascade and the suppression of the antiapoptotic protein Bcl-2 were both involved in the induction of apoptosis by $CdCl_2$. $CdCl_2$ at 30 μg/ml was also found to be cytotoxic to A549 cells but not to normal Wi38 cells. Higher concentrations reduced cell viability in both nonmalignant and malignant cells and ensured that their cytotoxic effects were present. This discovery could lead to a new perspective on the mechanism of action and potential applications of trace elements in treatment for cancer.

Financial support and sponsorship

Nil.

Conflicts of interest

There are no conflicts of interest.

References

1 Sinicropi MS, Amantea D, Caruso A, Saturnino C. Chemical and biological properties of toxic metals and use of chelating agents for the pharmacological treatment of metal poisoning. Arch Toxicol 2010; 84:501–520.

2 Friberg LT, Elinder GG, Kjellstrom T, Nordberg GF. Cadmium and health: a toxicological and epidemiological appraisal: Volume 2: effects and response (Vol. 1). Boca Raton, FL, USA: CRC Press; 2019.

3 Genchi G, Carocci A, Lauria G, Sinicropi MS, Catalano A. Nickel: human health and environmental toxicology. Int J Environ Res Public Health 2020; 17:679.

4 Hogervost J, Plusquin M, Vangronsvel J, Nawrot T, Cuypers A, Van Hecke E, *et al.* House dust as possible route ofenvironmental exposure to cadmium and lead in the adult general population. Environ Res 2007; 103:30–37.

5 Casado M, Anawar HM, Garcia-Sanchez A, Santa Regina I. Cadmium and zinc in polluted mining soils and uptake by plants (El Losar mine, Spain). Int Environ Poll 2008; 33: 146–159.

6 Tinkov AA, Filippini T, Ajsuvakovae OP, Skalnaya MG, Aaseth FJ, Bjorklundh G, *et al.* Cadmium and atherosclerosis: a review of toxicological mechanisms and a meta-analysis of epidemiologic studies. Environ Res 2018; 162:240–260.

7 Zhou Z, Wang C, Liu H, Huang Q, Wang M, Lei Y. Cadmium induced cell apoptosis, DNA damage, decreased DNA repair capacity, and genomic instability during malignant transformation of human bronchial epithelial cells. Int J Med Sci 2013; 10:1485–1496.

8 Pizzino G, Bitto A, Interdonato M, Galfo Z, Irrera N, Mecchio A, *et al.* Oxidative stress and DNA repair and detoxification gene expression in adolescents exposed to heavy metals living in the Milazzo-Valle del Melaarea (Sicily, Italy). Redox Biol 2014; 2:686–693.

9 Buha A, Matovic V, Antonijevic B, Bulat Z, Curcic M, Renieri EA, *et al.* Overview of cadmium thyroid disrupting effects and mechanisms. Int J Mol Sci 2018; 19:1501.

10 Zimtaa AA, Schitcub V, Gurzaud E, Stavarug C, Mandah G, Szedlacseki S, Berindan-Neagoe I. Biological and molecular modifications induced by cadmium and arsenic during breast and prostate cancer development. Environ Res 2019; 178:108700.

11 Sung H, Ferlay J, Siegel RL, Laversanne M, Soerjomataram I, Jemal A, Bray F. Global Cancer Statistics 2020: GLOBOCAN estimates of incidence and mortality worldwide for 36 cancers in 185 countries. CA Cancer J Clin 2021; 71:209–249.

12 Rashad Sh E, Abdel-TawabF M, Fahmy EM, Attallah AG, Ahmed ES, Haggran AA. Assessment of genotoxic effects of some food additives on some human cancer cells. Arab Univ J Agri Sci 2019; 27:1.

13 Rashad SHE, Abdel-Tawab FM, Fahmy EM, Attallah AG, Ahmed ES, Haggran AA. Application of the yeast comet assay in Testing some food additives for genotoxicity by comet assay in yeast. Egypt J Chem 2021; 64:7649–7667.

14 Bork U, Lee W, Kuchler A, Dittmar T, Thévenod F. Cadmium-induced DNA damage triggers G 2 / M arrest via chk1 / 2 and cdc2 in p53-deficient kidney proximal tubule cells. Am J Physiol Renal Physiol 2022; 23:255–265.

15 Rashad SHE, Haggran AA, Aboul-Elab EI, Shaalanc AH, Abdoond AS. Cytotoxic and genotoxic effects of 50nm Gold Nanorods on mouse splenocytes and human cell lines. Egypt J Chem 2022; Articles in Press.

16 Rashad SHE, Abdel-Tawab FM, Fahmy EM, Attallah AG, Ahmed ES, Haggran AA. Determination of genotoxic effects of some food additives on some human cancer cells by flow cytometry analysis. Egypt J Genet Cytol 2018; 47:329–343.

17 Livak KJ, Schmittgen TD. Analysis of relative gene expression data using real-time quantitative PCR and the 2 (–Delta Delta C (T)) method. Methods 2001; 25:402–408.

18 Mousa SHA, Haggran AA, Abou-El-Khier ZA, Sabry Sh M, Rashad Sh E. Assessment of cytotoxicity and genotoxicity response of zinc sulphate on eukaryotic cells. Egypt J Chem 2022; Articles in Press.

19 MOdewumi C, Latinwo LM, Sinclair A, Badisa VLD, Abdullah A, Badisa RB. Effect of cadmium on the expression levels of interleukin-1α and interleukin-10 cytokines in human lung cells. Mol Med Rep 2015; 12:6422–6426.

20 Forti E, Bulgheroni A, Cetin Y, Hartung T, Jennings P, Pfaller W, Prieto P. Characterisation of cadmium chloride induced molecular and functional alterations in airway epithelial cells. Cell Physiol Biochem 2010; 25:159–168.

21 Nemmiche S, Guiraud P. Cadmium-induced oxidative damages in the human BJAB cells correlate with changes in intracellular trace elements levels and zinc transporters expression. Toxicol In Vitro 2016; 37:169–177.

22 Skipper A, Sims JN, Yedjou CG, Tchounwou PB. Cadmium chloride induces DNA damage and apoptosis of human liver carcinoma cells via oxidative stress. Int J Environ Res Public Health 2016; 13:88.

23 Ravindran G, Chakrabarty D, Sarkar A. Cell specific stress responses of cadmium-induced cytotoxicity. Anim Cells Syst 2017; 21:23–30.

24 Luevano J, Damodaran C. A review of molecular events of cadmium-induced carcinogenesis. J Environ Pathol Toxicol Oncol 2014; 33:183–194.

25 Belliardo C, DiGiorgio C, Chaspoul F, Gallice P, Bergé-Lefranc D. Direct DNA interaction and genotoxic impact of three metals: cadmium, nickel and aluminium. J Chem Thermodynamics 2018; 125:271–277.

26 Karri V, Kumar V, Ramos D, Oliveira E, Schuhmacher M. Comparative in vitro toxicity evaluation of heavy metals (lead, cadmium, arsenic, and methylmercury) on HT-22 hippocampal cell line. Biol Trace Elem Res 2018; 184:226–239.